Multi-person Tracking by Multicut and Deep Matching

Siyu Tang(✉), Bjoern Andres, Mykhaylo Andriluka, and Bernt Schiele

Max Planck Institute for Informatics,
Saarbrücken Informatics Campus, Saarbrücken, Germany
tang@mpi-inf.mpg.de

Abstract. In Tang et al. (2015), we proposed a graph-based formulation that links and clusters person hypotheses over time by solving a minimum cost subgraph multicut problem. In this paper, we modify and extend Tang et al. (2015) in three ways: *(1)* We introduce a novel local pairwise feature based on local appearance matching that is robust to partial occlusion and camera motion. *(2)* We perform extensive experiments to compare different pairwise potentials and to analyze the robustness of the tracking formulation. *(3)* We consider a plain multicut problem and remove outlying clusters from its solution. This allows us to employ an efficient primal feasible optimization algorithm that is not applicable to the subgraph multicut problem of Tang et al. (2015). Unlike the branch-and-cut algorithm used there, this efficient algorithm used here is applicable to long videos and many detections. Together with the novel pairwise feature, it eliminates the need for the intermediate tracklet representation of Tang et al. (2015). We demonstrate the effectiveness of our overall approach on the MOT16 benchmark (Milan et al. 2016), achieving state-of-art performance.

1 Introduction

Multi person tracking is a problem studied intensively in computer vision. While continuous progress has been made, false positive detections, long-term occlusions and camera motion remain challenging, especially for people tracking in crowded scenes. Tracking-by-detection is commonly used for multi person tracking where a state-of-the-art person detector is employed to generate detection hypotheses for a video sequence. In this case tracking essentially reduces to an association task between detection hypotheses across video frames. This detection association task is often formulated as an optimization problem with respect to a graph: every detection is represented by a node; edges connect detections across time frames. The most commonly employed algorithms aim to find disjoint paths in such a graph [1–4]. The feasible solutions of such problems are sets of disjoint paths which do not branch or merge. While being intuitive, such formulations cannot handle the multiple plausible detections per person, which are generated from typical person detectors. Therefore, pre- and/or post-processing such as non maximum suppression (NMS) on the detections and/or the final tracks is performed, which often requires careful fine-tuning of parameters.

G. Hua and H. Jégou (Eds.): ECCV 2016 Workshops, Part II, LNCS 9914, pp. 100–111, 2016.
DOI: 10.1007/978-3-319-48881-3_8

The minimum cost subgraph multicut problem proposed in [5] is an abstraction of the tracking problem that differs conceptually from disjoint path methods. It has two main advantages: *(1)* Instead of finding a path for each person in the graph, it links and clusters multiple plausible person hypotheses (detections) jointly over time and space. The feasible solutions of this formulation are components of the graph instead of paths. All detections that correspond to the same person are clustered jointly within and across frames. No NMS is required, neither on the level of detections nor on the level of tracks. *(2)* For the multicut formulation, the costs assigned to edges can be positive, to encourage the incident nodes to be in the same track, or negative, to encourage the incident nodes to be in distinct tracks. Thus, the number and size of tracks does not need to be specified, constrained or penalized and is instead defined by the solution. This is fundamentally different also from distance-based clustering approaches, e.g. [6] where the cost of joining two detections is non-negative and thus, a non-uniform prior on the number or size of tracks is required to avoid a trivial solution. Defining or estimating this prior is a well-known difficulty. We illustrate these advantages in the example depicted in Fig. 1: We build a graph based on the detections on three consecutive frames, where detection hypotheses within and between frames are all connected. The costs assigned to the edges encourage the incident node to be in the same or distinct clusters. For simplicity, we only visualize the graph built on the detections of two persons instead of all. By solving the minimum cost subgraph multicut problem, a multicut of the edges is found (depicted as dotted lines). It partitions the graph into distinct components (depicted in yellow and magenta, resp.), each representing one person's track. Note that multiple plausible detections of the same person are clustered jointly, within and across frames.

The effectiveness of the multicut formulation for the multi person tracking task is driven by different factors: computing reliable affinity measures for pairs of detections; handling noisy input detections and utilizing efficient optimization methods. In this work, we extend [5] on those fronts. First, for a pair of detections, we propose a reliable affinity measure that is based an effective image matching method DeepMatching [7]. As this method matches appearance of local image regions, it is robust to camera motion and partial occlusion. In contrast, the pairwise feature proposed in [5] relies heavily on the spatio-temporal relations of tracklets (a short-term tracklet is used to estimate the speed of a person) which works well only for a static camera and when people walk with constant speed. By introducing the DeepMatching pairwise feature, we make the multicut formulation applicable to more general moving-camera videos with arbitrary motion of persons. Secondly, we eliminate the unary variables which are introduced in [5] to integrate the detection confidence into the multicut formulation. By doing so, we simplify the optimization problem and make it amenable to the fast Kernighan-Lin-type algorithm of [8]. The efficiency of this algorithm eliminates the need for an intermediate tracklet representation, which greatly simplifies the tracking pipeline. Thirdly, we integrate the detection confidence into the pairwise terms such that detections with low confidence simply have a low probability to be clustered with any other detection, most likely ending up as singletons that we remove in a post-processing step. With the above mentioned extensions, we are able to achieve competitive performance on the challenging MOT16 benchmark.

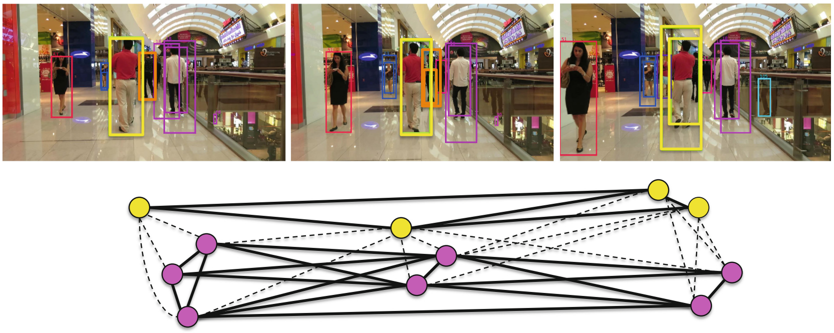

Fig. 1. An example for tracking by multicut. A graph (bottom) is built based on the detections in three frames (top). The connected components that are obtained by solving the multicut problem indicate the number of tracks (there are two tracks, depicted in yellow and magenta respectively) as well as the membership of every detection. (Color figure online)

2 Related Work

Recent work on multi-person tracking primarily focuses on tracking-by-detection. Tracking operates either by directly linking people detections over time [9,10], or by first grouping detections into tracklets and then combining those into tracks [11]. A number of approaches rely on data association methods such as the Hungarian algorithm [12,13], network flow optimization [4,11,14,15], and multiple hypotheses tracking [9], and combine them with novel ways to learn the appearance of tracked targets. [9] proposed to estimate a target-specific appearance model online and used a generic CNN representation to represent person appearance. In [12] it is proposed to formulate tracking as a Markov decision process with a policy estimated on the labeled training data. [16] proposes novel appearance representations that rely on the temporal evolution in appearance of the tracked target. In this paper we propose a pairwise feature that similarly to [10] is based on local image patch matching. Our model is inspired by [7] and it operates on pairs of hypotheses which allows to directly utilize its output as costs of edges on the hypothesis graph. Our pairwise potential is particularly suitable to our tracking formulation that finds tracks by optimizing a global objective function. This is in contrast to target-specific appearance methods that are trained online and require iterative assembly of tracks over time, which precludes globally solving for all trajectories in an image sequence.

Perhaps closest to our work are methods that aim to recover people tracks by optimizing a global objective function [5,14,17]. [17] proposes a continuous formulation that analytically models effects such as mutual occlusions, dynamics and trajectory continuity, but utilizes a simple color appearance model. [14] finds tracks by solving instances of a generalized minimum clique problem, but due to model complexity resorts to a greedy iterative optimization scheme that finds one track at a time whereas we jointly recover solutions for all tracks. We build on the multi-cut formulation proposed in [5] and generalize it to large scale sequences based on the extensions discussed below.

3 Multi-person Tracking as a Multicut Problem

In Sect. 3.1, we recall the minimum cost multicut problem that we employ as a mathematical abstraction for multi person tracking. We emphasize differences compared to the minimum cost subgraph multicut problem proposed in [5]. In Sect. 3.2, we define the novel DeepMatching feature and its incorporation into the objective function. In Sect. 3.3, we present implementation details.

3.1 Minimum Cost Multicut Problem

In this work, multi person tracking is cast as a minimum cost multicut problem [18] w.r.t. a graph $G = (V, E)$ whose node V are a finite set of *detections*, i.e., bounding boxes that possibly identify people in a video sequence. Edges within and across frames connect detections that possibly identify the same person. For every edge $vw \in E$, a cost or reward $c_{vw} \in \mathbb{R}$ is to be payed if and only if the detections v and w are assigned to distinct tracks. Multi person tracking is then cast as a binary linear program

$$\min_{x \in \{0,1\}^E} \quad \sum_{e \in E} c_e x_e \tag{1}$$

$$\text{subject to} \quad \forall C \in \text{cycles}(G) \ \forall e \in C : \ x_e \leq \sum_{e' \in C \setminus \{e\}} x_{e'} . \tag{2}$$

Note that the costs c_e can be both positive or negative. For detections $v, w \in V$ connected by an edge $e = \{v, w\}$, the assignment $x_e = 0$ indicates that v and w belong to the same track. Thus, the constraints (2) can be understood as follows: If, for any neighboring nodes v and w, there exists a path in G from v to w along which all edges are labeled 0 (indicating that v and w belong to the same track), then the edge vw cannot be labeled 1 (which would indicate the opposite). In fact, (2) are generalized transitivity constraints which guarantee that a feasible solution x well-defines a decomposition of the graph G into tracks.

We construct the graph G such that edges connect detections not only between neighboring frames but also across longer distances in time. Such edges $vw \in E$ allow to assign the detections v and w to the same track even if there would otherwise not exist a vw-path of detections, one in each frame. This is essential for tracking people correctly in the presence of occlusion and missing detections.

Differences compared to [5]**.** The minimum cost multicut problem (1) and (2), we consider here differs from the minimum cost subgraph multicut problem of [5]. In order to handle false positive detections, [5] introduces additional binary variables at the nodes, switching detections on or off. A cost of switching a detection on is defined w.r.t. a confidence score of that detection. Here, we do not consider binary variables at nodes and incorporate a detection confidence into the costs of edges. In order to remove false positive detections, we remove small clusters from the solution in a post-processing step. A major advantage of this modification is that our minimum cost multicut problem (1) and (2), unlike the minimum cost subgraph multicut problem of [5], is amenable to efficient approximate optimization by means of the KLj algorithm [8], without any modification.
This algorithm, unlike the branch-and-cut algorithm of [5], can be applied in practice directly to the graph of detections defined above, thus eliminating the need for the smaller intermediate representation of [5] by tracklets.

Optimization. Here, we solve instances of the minimum cost multicut problem approximatively with the KLj algorithm [8]. This algorithm iteratively updates bipartitions of a subgraph. The worst-case time complexity of any such update is $O(|V||E|)$. The number of updates is not known to be polynomially bounded but is small in practice (less than 30 in our experiments). Moreover, the bound $O(|V||E|)$ is almost never attained in practice, as shown by the more detailed analysis in [8].

3.2 Deep Matching Based Pairwise Costs

In order to specify the costs of the optimization problem introduced above for tracking, we need to define, for any pair of detection bounding boxes, a cost or reward to be payed if these bounding boxes are assigned to the same person. For that, we wish to quantify how likely it is that a pair of bounding boxes identify the same person. In [5], this is done w.r.t. an estimation of velocity that requires an intermediate tracklet representation and is not robust to camera motion. Here, we define these costs exclusively w.r.t. image content. More specifically, we build on the significant improvements in image matching made by DeepMatching [7].

DeepMatching applies a multi-layer deep convolutional architecture to yield possibly non-rigid matchings between a pair of images. Figure 2 shows results of DeepMatching for two pairs of images from the MOT16 sequences[1]. The first pair of images is taken by a moving camera; the second pair of images is taken by a static camera. Between both pairs of images, matched points (blue arrows) relate a person visible in one image to the same person in the second image.

Next, we describe our features defined w.r.t. a matching of points between a pair of detection bounding boxes. Each detection bounding box $v \in V$ has the

[1] We use the visualization code provided by the authors of [7].

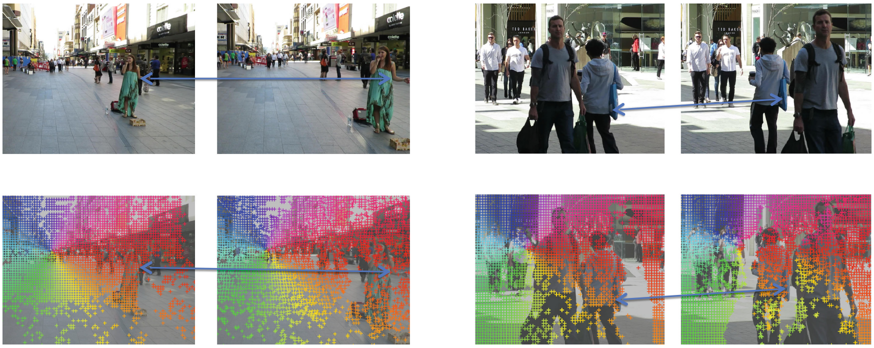

Fig. 2. Visualization of the DeepMatching results on the MOT16 sequences. (Color figure online)

following properties: its spatio-temporal location (t_v, x_v, y_v), scale h_v, detection confidence ξ_v and, finally, a set of keypoints M_v inside v. Given two detection bounding boxes v and w connected by the edge $\{v, w\} = e \in E$, we define $MU = |M_v \cup M_w|$ and $MI = |M_v \cap M_w|$ and the five features

$$f_1^{(e)} := MI/MU \tag{3}$$

$$f_2^{(e)} := \min\{\xi_v, \xi_w\} \tag{4}$$

$$f_3^{(e)} := f_1^{(e)} f_2^{(e)} \tag{5}$$

$$f_4^{(e)} := (f_1^{(e)})^2 \tag{6}$$

$$f_5^{(e)} := (f_2^{(e)})^2 \tag{7}$$

Given, for any edge $e = \{v, w\} \in E$ between two detection bounding boxes v and w, the feature vector $f^{(e)}$ for this pair, we learn a probability $p_e \in (0, 1)$ of these detection bounding boxes to identify the same person. More specifically, we assume that p_e depends on the features $f^{(e)}$ by a logistic form

$$p_e := \frac{1}{1 + \exp(-\langle \theta, f^{(e)} \rangle)} \tag{8}$$

with parameters θ. We estimate these parameters from training data by means of logistic regression. Finally, we define the cost c_e in the objective function (1) as

$$c_e := \log \frac{p_e}{1 - p_e} = \langle \theta, f^{(e)} \rangle. \tag{9}$$

Two remarks are in order: Firstly, the feature $f_2^{(e)}$ incorporates the detection confidences of v and w that defined unary costs in [5] into the feature $f^{(e)}$ of the pair $\{v, w\}$ here. Consequently, detections with low confidence will be assigned with low probability to any other detection. Secondly, the features $f_3^{(e)}, f_4^{(e)}, f_5^{(e)}$ are to learn a non-linear map from features $f_1^{(e)}, f_2^{(e)}$ to edge probabilities by means of linear logistic regression.

3.3 Implementation Details

Clusters to tracks. The multicut formulation clusters detections jointly over space and time for each target. It is straight-forward to generate tracks from such clusters: In each frame, we obtain a representative location (x, y) and scale h by averaging all detections that belong to the same person (cluster). A smooth track of the person is thus obtained by connecting these averages across all frames. Thanks to the pairwise potential incorporating a detection confidence, low confidence detections typically end up as singletons or in small clusters which are deleted from the final solution. Specifically, we eliminate all clusters of size less than 5 in all experiments.

Maximum temporal connection. Introducing edges that connect detections across longer distance in time is essential to track people in the presence of occlusion. However, with the increase of the distance in time, the pairwise feature becomes less reliable. Thus, when we construct the graph, it is necessary to set a maximum distance in time. In all the experiments, we introduce edges for the detections that are at most 10 frames apart. This parameter is based on the experimental analysis on the training sequences and is explained in more detail in Sect. 4.1.

4 Experiments and Results

We analyze our approach experimentally and compare to prior work on the MOT16 Benchmark [19]. The benchmark includes training and test sets composed of 7 sequences each. We learn the model parameters for the test sequences based on the corresponding training sequences. We first conduct an experimental analysis that validates the effectiveness of the DeepMatching based affinity measure in Sect. 4.1. In Sect. 4.2 we demonstrate that the multicut formulation is robust to detection noise. In Sect. 4.3 we compare our method with the best published results on the MOT16 Benchmark.

4.1 Comparison of Pairwise Potentials

Setup. In this section we compare the DeepMatching (DM) based pairwise potential with a conventional spatio-temporal relation (ST) based pairwise potential.

More concretely, given two detections v and w, each has the following properties: spatio-temporal location (t, x, y), scale h, detection confidence ξ. Based on these properties the following auxiliary variables are introduced to capture geometric relations between the bounding boxes: $\Delta x = \frac{|x_v - x_w|}{\bar{h}}$, $\Delta y = \frac{|y_v - y_w|}{\bar{h}}$, $\Delta h = \frac{|h_v - h_w|}{\bar{h}}$, $y = \frac{|y_v - y_w|}{\bar{h}}$, $IOU = \frac{|B_v \cap B_w|}{|B_v \cup B_w|}$, $t = t_v - t_w$, where $\bar{h} = \frac{(h_v + h_w)}{2}$, IOU is the intersection over union of the two detection bounding box areas and ξ_{min} is the minimum detection score between ξ_v and ξ_w. The pairwise feature $f^{(e)}$ for the spatio-temporal relations (ST) is then defined as $(\Delta t, \Delta x, \Delta y, \Delta h, IOU, \xi_{min})$. Intuitively, the ST features are able to provide useful information within a short temporal window, because they only model the geometric relations between bounding boxes. DM is built upon matching of local image features that is reliable for camera motion and partial occlusion in longer temporal window.

We collect test examples from the MOT16-09 and MOT16-10 sequences which are recorded with a static camera and a moving camera respectively. The positive (negative) pairs of test examples are the detections that are matched to the same (different) persons' ground truth track over time. The negative pairs also include the false positive detections on the background.

Metric. The metric is the verification accuracy, the accuracy or rate of correctly classified pairs. For a pair of images belong to the same (different) person, if the estimated joint probability is larger (smaller) than 0.5, the estimation is considered as correct. Otherwise, it is a false prediction.

Results. We conduct a comparison between the accuracy of the DM feature and the accuracy of the ST feature as a function of distance in time. It can be seen from Table 1 that the ST feature achieves comparable accuracy only up to 2 frames distance. Its performance deteriorates rapidly for connections at longer time. In contrast, the DM feature is effective and maintains superior accuracy over time. For example on the MOT16-10 sequence which contains rapid camera motion, the DM feature improves over the ST feature by a large margin after 10 frames and it provides stable affinity measure even at 20 frames distance (accuracy = 0.925). On the MOT16-09 sequence, the DM feature again shows superior accuracy than the ST feature starting from $\triangle t = 2$. However, the accuracy of the DM feature on the MOT16-09 is worse than the one on MOT16-10, suggesting the quite different statistic among the sequences from the MOT16 benchmark. As discussed in Sect. 3.3, it is necessary to set a maximum distance in time to exclude unreliable pairwise costs. Aiming at a unique setting for all sequences, we introduce edges for the detections that are maximumly 10 frames apart in the rest experiments of this paper.

Table 1. Comparison of tracking results based on the DM and the ST feature. The metic is the accuracy or rate of correctly classified pairs on the MOT16-09 and the MOT16-10 sequences.

MOT16-09: static camera						
Feature	$\triangle t = 1$	$\triangle t = 2$	$\triangle t = 5$	$\triangle t = 10$	$\triangle t = 15$	$\triangle t = 20$
ST	0.972	0.961	0.926	0.856	0.807	0.781
DM	0.970 (−0.2 %)	0.963 (+0.2 %)	0.946 (+2 %)	0.906 (+5 %)	0.867 (+6 %)	0.820 (+3.9 %)
MOT16-10: moving camera						
Feature	$\triangle t = 1$	$\triangle t = 2$	$\triangle t = 5$	$\triangle t = 10$	$\triangle t = 15$	$\triangle t = 20$
ST	0.985	0.977	0.942	0.903	0.872	0.828
DM	0.985	0.984 (+0.7 %)	0.975 (+3.3 %)	0.957 (+5.4 %)	0.939 (+6.7 %)	0.925 (+9.7 %)

Table 2. Tracking performance on different sets of input detections. $Score_{\min}$ indicates the minimum detection score threshold. $|V|$ and $|E|$ are the number of nodes (detections) and edges respectively.

MOT16-09							
$Score_{\min}$	$-\infty$	-0.3	-0.2	-0.1	0	0.1	1
$\|V\|$	5377	4636	4320	3985	3658	3405	1713
$\|E\|$	565979	422725	367998	314320	265174	229845	61440
Run time (s)	30.48	19.28	13.46	11.88	8.39	6.76	1.71
MOTA	37.9	43.1	43.1	44.9	45.8	44.1	34.1
MOT16-10							
$Score_{\min}$	$-\infty$	-0.3	-0.2	-0.1	0	0.1	1
$\|V\|$	8769	6959	6299	5710	5221	4823	2349
$\|E\|$	1190074	755678	621024	511790	427847	365949	88673
Run time (s)	88.34	39.28	30.08	21.99	16.13	13.66	1.94
MOTA	26.8	32.4	34.4	34.5	34.5	33.9	23.3

Table 3. Tracking performance on MOT16.

Method	MOTA	MOTP	FAF	MT	ML	FP	FN	ID Sw	Frag	Hz	Detector
NOMT [10]	46.4	76.6	1.6	18.3 %	41.4 %	9753	87565	359	504	2.6	Public
MHT [9]	42.8	76.4	1.2	14.6 %	49.0 %	7278	96607	462	625	0.8	Public
CEM [17]	33.2	75.8	1.2	7.8 %	54.4 %	6837	114322	642	731	0.3	Public
TBD [21]	33.7	76.5	1.0	7.2 %	54.2 %	5804	112587	2418	2252	1.3	Public
Ours	46.3	75.7	1.09	15.5 %	39.7 %	6449	90713	663	1115	0.8	Public

4.2 Robustness to Input Detections

Handling noisy detection is a well-known difficulty for tracking algorithms. To assess the impact of the input detections on the tracking result, we conduct tracking experiments based on different sets of input detections that are obtained by varying a minimum detection score threshold ($Score_{min}$). For example, in Table 2, $Score_{min} = -\infty$ indicates that all the detections are used as tracking input; whereas $Score_{min} = 1$ means that only the detections whose score are equal or larger than 1 are considered. Given the fact that the input detections are obtained from a DPM detector [20], $Score_{min} = -\infty$ and $Score_{min} = 1$ are the two extreme cases, where the recall is maximized for the former one and high precision is obtained for the latter one.

Metric. We evaluate the tracking performance of the multicut model that operates on different sets of input detections. We use the standard CLEAR MOT metrics. For simplicity, in Table 2 we report the Multiple Object Tracking Accuracy (MOTA) that is a cumulative measure that combines the number of False Positives (FP), the number of False Negatives (FN) and the number of ID Switches (IDs).

Results. On the MOT16-09 sequence, when the minimum detection score threshold ($Score_{min}$) is changed from 0.1 to -0.3, the number of detection is largely increased (from 3405 to 4636), however the MOTA is only decreased by 1 percent (from 44.1 % to 43.1 %). Even for the extreme cases, where the detections are either rather noisy ($Score_{min} = -\infty$) or sparse ($Score_{min} = 1$), the MOTAs are still in the reasonable range. The same results are found on the MOT16-10 sequence as well. Note that, for all the experiments, we use the same parameters, we delete the clusters whose size is smaller than 5 and no further tracks splitting/merging is performed.

These experiments suggest that the multicut formulation is very robust to the noisy detection input. This nice property is driven by the fact that the multicut formulation allows us to jointly cluster multiple plausible detections that belong to the same target over time and space.

We also report run time in Table 2. The KLj multicut solver provides arguably fast solution for our tracking problem. E.g. for the problem with more than one million edges, the solution is obtained in 88.34 s. Detailed run time analysis of the KLj algorithm are shown in [8].

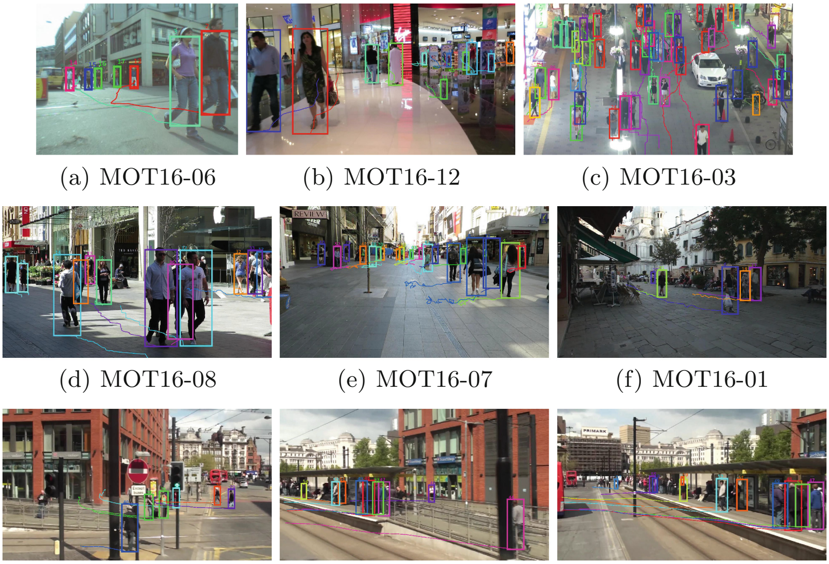

(a) MOT16-06 (b) MOT16-12 (c) MOT16-03

(d) MOT16-08 (e) MOT16-07 (f) MOT16-01

(g) MOT16-09 (frame 290) (h) MOT16-09 (frame 360) (i) MOT16-09 (frame 390)

Fig. 3. Qualitative results for all the sequences from the MOT16 Benchmark. The first and second rows are the results from the MOT16-01, MOT16-03, MOT16-06, MOT16-07, MOT16-08 and MOT16-12 sequence. The third row is the result from the MOT16-14 sequence when the camera mounted on a bus is turning fast at a street intersection.

4.3 Results on MOT16

We test our tracking model on all the MOT16 sequences and submitted our results to the ECCV 2016 MOT Challenge [2] for evaluation. The performance is shown in Table 3. The detailed performance and comparison on each sequence will be revealed at the ECCV 2016 MOT Challenge Workshop. We compare our method with the best reported results including NOMT [10], MHT-DAM [9], TBD [21] and CEM [17]. Overall, we achieve the second best performance in terms of MOTA with 0.1 point below the best performed one [10]. We visualize our results in Fig. 3. On the MOT16-12 and MOT16-07 sequences, the camera motion is irregular; whereas on the MOT16-03 and MOT16-08 sequences, scenes are crowded. Despite these challenges, we are still able to link people through occlusions and produce long-lived tracks. The third row of Fig. 3 shows images captured by a fast moving camera mounted on a bus turning at a street intersection. Under such extreme circumstance, our model is able to track people in a stable and persistent way, demonstrating the reliability of the multicut formulation for multi-person tracking task.

5 Conclusion

In this work, we revisit the multi-cut approach for multi-target tracking that is proposed in [5]. We propose a novel pairwise potential that is built based on local image patch appearance matching. We demonstrate extensive experimental analysis and show state-of-art tracking performance on the MOT16 Benchmark. In the future we plan to further develop our approach by incorporating long-range temporal connections in order to deal with longer-term occlusions, and will extend the model with more powerful pairwise terms capable of matching person hypothesis over longer temporal gaps.

Acknowledgements. This work has been supported by the Max Planck Center for Visual Computing and Communication.

References

1. Pirsiavash, H., Ramanan, D., Fowlkes, C.C.: Globally-optimal greedy algorithms for tracking a variable number of objects. In: CVPR (2011)
2. Segal, A.V., Reid, I.: Latent data association: Bayesian model selection for multi-target tracking. In: ICCV (2013)
3. Andriluka, M., Roth, S., Schiele, B.: People-tracking-by-detection and people-detection-by-tracking. In: CVPR (2008)
4. Zhang, L., Li, Y., Nevatia, R.: Global data association for multi-object tracking using network flows. In: CVPR (2008)
5. Tang, S., Andres, B., Andriluka, M., Schiele, B.: Subgraph decomposition for multi-target tracking. In: CVPR (2015)

[2] https://motchallenge.net/workshops/bmtt2016/eccvchallenge.html.

6. Wen, L., Li, W., Yan, J., Lei, Z., Yi, D., Li, S.Z.: Multiple target tracking based on undirected hierarchical relation hypergraph. In: CVPR, June 2014
7. Weinzaepfel, P., Revaud, J., Harchaoui, Z., Schmid, C.: DeepFlow: large displacement optical flow with deep matching. In: ICCV (2013)
8. Keuper, M., Levinkov, E., Bonneel, N., Lavoué, G., Brox, T., Andres, B.: Efficient decomposition of image and mesh graphs by lifted multicuts. In: ICCV (2015)
9. Kim, C., Li, F., Ciptadi, A., Rehg, J.M.: Multiple hypothesis tracking revisited. In: ICCV (2015)
10. Choi, W.: Near-online multi-target tracking with aggregated local flow descriptor. In: ICCV (2015)
11. Wang, B., Wang, G., Chan, K.L., Wang, L.: Tracklet association by online target-specific metric learning and coherent dynamics estimation (2015). arXiv:1511.06654
12. Xiang, Y., Alahi, A., Savarese, S.: Learning to track: online multi-object tracking by decision making. In: ICCV (2015)
13. Bewley, A., Ge, Z., Ott, L., Ramos, F., Upcroft, B.: Simple online and realtime tracking (2016). arXiv:1602.00763
14. Roshan Zamir, A., Dehghan, A., Shah, M.: GMCP-tracker: global multi-object tracking using generalized minimum clique graphs. In: Fitzgibbon, A., Lazebnik, S., Perona, P., Sato, Y., Schmid, C. (eds.) ECCV 2012, Part II. LNCS, vol. 7573, pp. 343–356. Springer, Heidelberg (2012)
15. Li, Y., Huang, C., Nevatia, R.: Learning to associate: hybrid boosted multi-target tracker for crowded scene. In: CVPR (2009)
16. Yang, M., Jia, Y.: Temporal dynamic appearance modeling for online multi-person tracking. arXiv preprint (2015). arXiv:1510.02906
17. Milan, A., Roth, S., Schindler, K.: Continuous energy minimization for multitarget tracking. IEEE TPAMI **36**(1), 58–72 (2014)
18. Chopra, S., Rao, M.: The partition problem. Math. Program. **59**(1–3), 87–115 (1993)
19. Milan, A., Leal-Taixé, L., Reid, I.D., Roth, S., Schindler, K.: MOT16: a benchmark for multi-object tracking (2016). arXiv:1603.00831
20. Felzenszwalb, P.F., Girshick, R.B., McAllester, D., Ramanan, D.: Object detection with discriminatively trained part-based models. IEEE TPAMI **32**(9), 1627–1645 (2010)
21. Geiger, A., Lauer, M., Wojek, C., Stiller, C., Urtasun, R.: 3d traffic scene understanding from movable platforms. IEEE TPAMI **36**(5), 1012–1025 (2014)